IFSCC 2025 full paper ( IFSCC2025-1113 )

# *"A Powerful Collagen Supramolecular Vehicle to Amplify the Skin Regenerative Effects of Actives"*

**Jingui Zhang [1], Liyun Hu [1], Chijian Zhang [1], Yongjie Lu [2], Zhiting Zhang [2,*], Qiyin Liu [2], Xian Xu [2], Li Ye [3,4], Dongcui Li [2]**

[1] Guangdong C1 Life Biotech Co., Ltd., Guangzhou, China; [2] Hua An Tang Biotech Group Co., Ltd., Guangzhou, China; [3] Dermatology Hospital, Southern Medical University, Guangzhou, Guangdong, China; [4] Hygiene Detection Center,School of Public Health, Southern Medical University (NMPA Key Laboratory for Safety Evaluation of Cosmetics, Guangdong Provincial Key Laboratory of Tropical Disease Research), Guangzhou, Guangdong, China

## 1. Introduction

Collagen is a fibrillar protein and a major component of the extracellular matrix (ECM) in the dermis. By providing structural firmness, collagen plays a crucial role in maintaining the youthful and attractive appearance of the skin, making it a promising anti-aging ingredient in cosmetic applications [1]. In recent years, biomaterials derived from biomolecules have been extensively developed, facilitating advances in therapeutics, drug delivery, diagnosis, tissue engineering [2]. It is widely recognized that the molecular building blocks of life possess sophisticated recognition properties, and biomaterials designed based on these structures may exhibit remarkable and unexpected functionalities.

With the rapid development of recombinant collagen technologies, particularly recombinant human collagen type III (rhCol III), the application of collagen in skincare has been greatly expanded [3, 4]. Current research efforts primarily focus on engineering recombinant human collagen through synthetic biology approaches, such as the incorporation of functional peptide fragments to enhance intrinsic biological activities for direct cosmetic use. Among these, rhCol has attracted considerable attention due to its similarity to native dermal collagen and its superior biocompatibility and regenerative properties. Moreover, rhCol, composed of amino acids and peptides, offers abundant structural cavities that can accommodate the binding of small molecules， thereby enabling the formation of novel complexes. However, despite these advances, most studies have concentrated on utilizing collagen itself as a functional ingredient, while little attention has been paid to leveraging its binding sites for the conjugation and co-delivery of bioactive compounds. This strategy, which could potentially create synergistic effects and broaden the functional scope of collagen-based materials, remains largely unexplored in the skincare field. These properties suggest that rhCol holds great promise not only as an anti-aging component but also as a versatile vehicle for the innovative design of biomaterials and skin care strategies.

Spermidine (SPD) is a naturally occurring biogenic polyamine known for its significant health benefits [5]. Acting as a key signaling molecule, SPD effectively induces autophagy through

multiple pathways, including regulation at the genetic and protein levels, as well as modulation of inflammation [6]. Autophagy is an intrinsic degradation mechanism, clears damaged or senescent organelles, thereby rejuvenating the cellular microenvironment and supporting normal cellular activities, ultimately contributing to anti-aging effects and lifespan extension. Ergothioneine (EGT) is a naturally occurring amino acid with potent antioxidant properties particularly targeting the mitochondria. EGT exerts protective effects against oxidative stress, reducing damage to DNA, proteins and lipid caused by oxidative stimuli [7]. Accordingly, EGT has become a popular ingredient in skin care formulations targeting anti-aging.

In this study, we aimed to design an innovative supramolecular biomaterial based on recombinant collagen for the conjugation and delivery of small molecules, thereby exploring novel functional applications. Specifically, we developed a modified rhCol by introducing a leader peptide to enhance its permeation across biological barriers and facilitate binding with bioactive compounds. Building upon this framework, we constructed a rhCol–spermidine (SPD) complex, designated as ColMax, serving as a supramolecular vehicle to boost the delivery and efficacy of small molecule actives. Ergothioneine (EGT) was selected as a model molecule to further evaluate the capacity of ColMax in enhancing skin regeneration and cellular rejuvenation. The ColMax-EGT combination was subsequently prepared, and its synergistic effects on cellular functions were investigated. An AI-driven molecular docking platform and quartz crystal microbalance with dissipation (QCM-D) analysis were employed to verify the interactions between rhCol and the small molecules. In vitro assessments demonstrated that ColMax exhibited a synergistic amplification of biological activities, revealing new potential applications for collagen-based biomaterials in skin repair and rejuvenation.

## 2. Materials and Methods

### *2.1. Materials*

Luria-Bertani medium (LB), One-Step PAGE Gel Fast Preparation Kit (12%), BCA Protein Quantification Kit, 2-Amino-2-(hydroxymethyl)-1,3-propanediol (Tris (hydroxymethyl) aminomethane, Tris base, Trizma base), Tris (hydroxymethyl) aminomethane hydrochloride (Tris-HCl), Dulbecco's modified eagle medium (DMEM), Phosphate Buffered Saline (PBS), Trypsin-EDTA solution, Epidermal Growth Factor (Animal-free recombinant human EGF), Fetal Bovine Serum (FBS), RaPure Total RNA Kit, HiScript II Q RT SuperMix for qPCR(+gDNA wiper), PowerUp™ SYBR™ Green Master Mix, Lipopolysaccharide (LPS), Dexamethasone (DXMS), Complete culture medium for human skin fibroblasts, Hanks' Balanced Salt Solution (HBSS), DAPGreen-Autophagy Detection Kit, NucBlue™ Live ReadyProbes™ Kit were purchased from standard commercial suppliers. All other reagents used were of analytical purity or higher.

*Escherichia coli (E. coli)* BL21 (DE3) strain was used for recombinant protein expression, Human immortalized epidermal keratinocytes (HaCaT), human acute monocytic macrophage leukemia cells (THP-1), and normal human dermal fibroblasts (NHDF) were used for cellular experiments. All cells employed in this study were immortalized cell lines.

### *2.2. Synthesis of Recombinant Human Collagen Type III*

A functional fragment from the triple-helix region of human type III collagen, along with a sequence derived from the globular propeptide domain of human type III procollagen, was selected for recombinant construction. Using bioengineering techniques, a leader peptide sequence and two tandem repeats of the functional fragment were inserted into a plasmid

vector, which was subsequently transformed into *E. coli* for expression. The rhCol III was obtained through fermentation, followed by purification processes. The purified protein was dissolved in Tris-HCl buffer and stored at 4 °C. The concentration of rhCol III was determined using the BCA assay.

### *2.3. In Vitro Permeability Test*

The in vitro skin permeability of rhCol III was evaluated using Strat-M® membranes mounted between the donor and receptor compartments of a vertical Franz diffusion cell. The receptor compartment was filled with 8 mL of buffer solution, maintained at 32 °C with continuous stirring at 300 rpm. A 1.5 mL aliquot of the rhCol III sample was added to the donor compartment. At predetermined time points (3, 6, 12, and 24 hours), 1 mL of solution was withdrawn from the receptor compartment and replaced with fresh buffer. The protein concentration of each sample was measured using the BCA assay, and the cumulative permeation per unit area was calculated and plotted against time to assess the transdermal delivery efficiency of rhCol III.

### *2.4. Complexation Prediction by Molecular Docking*

The triple helix structure of rhCol III was first simulated using Alphafold3 (AF3) (https://alphafoldserver.com/). Molecular docking was subsequently performed using Autodock Vina (https://vina.scripps.edu/downloads/) to analyze the interaction between rhCol III and ligands including SPD, EGT and other bioactive molecules, with their respective structures obtained from PubChem (https://pubchem.ncbi.nlm.nih.gov/). The binding sites and binding energy were evaluated to predict the complexation of rhCol with these molecules. The docking results were visualized using Pymol (https://www.cgohlke.com/) to examine the interaction at a molecular level.

### *2.5. Quartz Crystal Microbalance with Dissipation (QCM-D)*

QCM-D measurements were employed to investigate the real-time adsorption and desorption behavior of rhCol from a SPD solution. Experiments were conducted using a Q-Sense E4 system (Biolin Scientific AB, Sweden) equipped with a standard flow module and standard gold QSX 301 sensors. rhCol and SPD were prepared by diluting with glycerol and Tris-HCl solution. In the experimental procedure, sensors were first mounted in the QCM-D system, and a stable baseline was established by flowing glycerol and Tris-HCl solution at a rate of 100 µL/min for 2 minutes. The temperature of the chambers was maintained at 37℃. Once the baseline was stabilized, the rhCol solution was introduced into the flow cell, and the adsorption was allowed for 30 minutes. This was followed by a 10-minute wash with glycerol and Tris-HCl solution, and a 12-min wash with SPD solution. Frequency and dissipation changes of the odd harmonics were continuously monitored and recorded in real-time to track the adsorption and desorption processes.

### *2.6. Preparation of rhCol-SPD Supramolecular Complex*

rhCol and SPD were mixed in Tris-HCl buffer at different mass ratios (1:1, 2:1, 5:1, 10:1, 20:1, 100:1). The mixture was stirred at room temperature to ensure uniform distribution of the components. After the reaction, the resulting products were sealed and stored at 4℃ for further use.

### *2.7. Cell Autophagy Assay*

Normal human dermal fibroblast (NHDF) cells were seeded in a 96-well plate with black walls and transparent caps, and cultured for 24 hours. After discarding the original culture medium, the cells were washed once with complete medium and incubated with DAPGreen working solution for 30 minutes. Following incubation, the DAPGreen losution was discarded, and the cells were washed twice with complete medium before being incubated for an additional 16 hours. The culture medium was then replaced, with complete medium for the negative control (NC), serum-free medium for the positive control (PC), and the samples added to the experimental groups. After 24 hours of incubation, the staining solution was removed and replaced with HBSS, and fluorescence images were captured for each well. The relative fluorescence intensity per well was calculated and anaylzed statistically.

### *2.8. Cell Migration Assay*

HaCaT cells were seeded to a 96-well plate and incubated in a carbon dioxide incubator for 24 hours. An automatic scratch instrument was then used to create a "wound" by making scratches on the surface of the wells. The plate was washed three times with PBS, and serum-free medium containing the sample to be tested was added to the wells. EGF was added to the positive control group (PC), and the samples were added to the experimental groups. After the addition of samples, images of the scratch were immediately captured under a microscope at 0 hours. The plate was thenincubated for 15 hours, and images were taken again to record changes in the scratch area. The scratch area was quantified from the images, and the healing rates were compared between NC and each experimental group to evaluate the effects of the samples on cell migration.

### *2.9. Pro-inflammatory Cytokine Expression*

THP-1 cells and the samples were added to a 24-well plate and cultured for 24 hours. The experimental setup include a negative control group (NC), model group (M), positive control group (PC) and sample group (Sn). Dexamethasone was added to the PC group, while the samples to be tested were added to Sn groups. LPS was added to the M group, PC group, and Sn groups, and the cells were incubated for an additional 24 hours. After incubation, cells from each group were collected, and total RNA was extracted. The RNA was reverse transcribed into cDNA, and the relative expression level of the pro-inflammatory cytokine *TNF-α* was quantified by qPCR, with *GAPDH* as the internal reference gene.

## 3. Results

### *3.1. Synthesis and Optimization of rhCol III*

The triple helix structure region of type III collagen is composed of repeated G-X-Y, where G is glycine (GLY), X and Y can be any amino acids. However, X is usually proline (PRO), and Y is usually hydroxyproline (HYP). PRO and HYP belong to imino acids. Since both PRO and HYP are rigid cyclic amino acids, they restrict the rotation of the main chain of the polypeptide, thereby contributing to the stability of the triple helix [8, 9].

As shown in Figure 1, we selected a functional fragment from the triple helix structure of rhCol. It is the first of a long, non-imino acid-containing sequence of a native collagen triple helix. The looser superhelical structure of the central non-imino acid-containing region combined with the extra contacts afforded by ionic and polar residues likely play a role in fibrillar assembly and interactions with other extracellular components [10]. The imino acid-rich regions at both ends of this fragment have tight superhelical structure, which contributes to

the stability of rhCol. Furthermore, the GLY-PRO-HYP structure of this fragment can make the triple helix structure more stable [11]. This phenomenon is very interesting. It's like the two ends of three ropes are tied tightly, and the middle part interacts more freely with the outside world without affecting the overall stability. We also selected a sequence from the spherical propeptide of human type III procollagen and named it leader peptide. This structure is rich in polar amino acids, which can be used as a carrier to combine with bioactive small molecules.

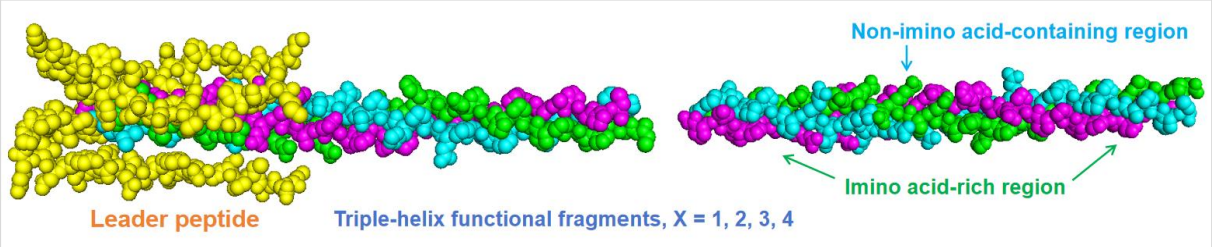


**Figure 1.** Schematic illustration of designed rhCol structure and the example shown here is X=2.

To optimize rhCol, we combined the leader peptides with 1, 2, 3, and 4 repetitive functional fragments using bioengineering techniques and compared their efficacy in various cell-based assays. After screening through multiple cell models, the rhCol with the functional fragment repeated twice demonstrated the strongest overall performance. As shown in the cell migration results in Figure 2a, this candidate exhibited the best cell scratch repair effect, along with other data (not shown here) supporting its superior efficacy. Additionally, the permeability test results in Figure 2b indicate that this rhCol candidate, with the fragment repeated twice, has excellent transdermal permeability, further enhancing its efficacy.

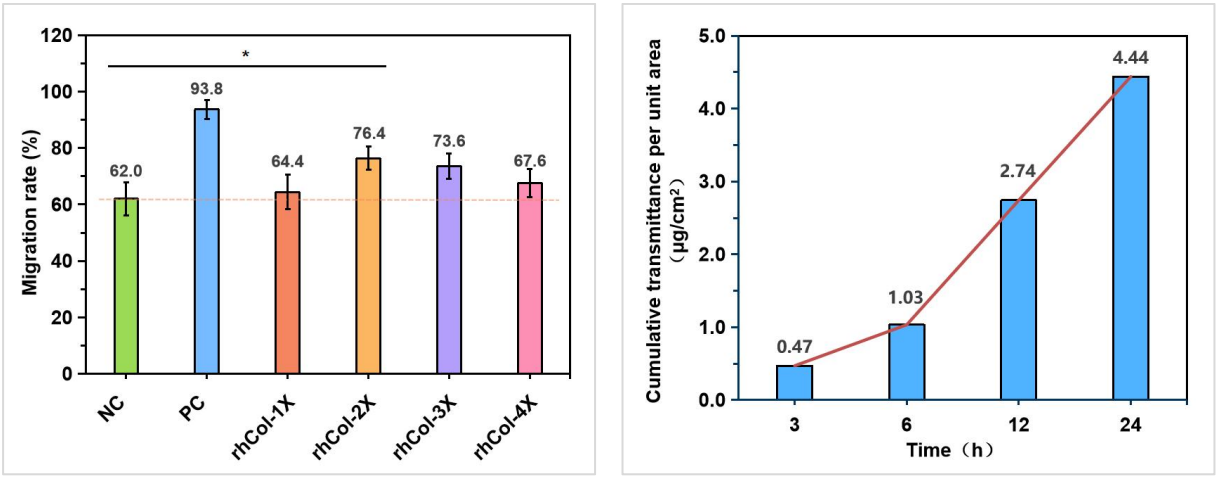


(**a**) (**b**)

**Figure 2.** Cell migration and permeability results of rhCol. (a) Cell migration rates of rhCol with different repetitions of the functional fragment (n = 2; *p < 0.05). (b) Permeability results of best candidate rhCol with the functional fragment repeated twice.

### *3.2. Complexation of rhCol-SPD (ColMax) by Molecular Docking*

AF3 is the latest generation of protein structure prediction tool, capable of predicting the structure and interaction of proteins, DNA, RNA and some small ligands with unprecedented accuracy [12]. We used AF3 to predict the triple helix structure of the optimized rhCol candidate. The 3D structure predicted by AlphaFold3 is shown in Figure 3a. To our surprise, it resembled a triangular arrow. In the triple helical structure region, areas rich in imino acids form tight triple helices, while regions containing non-amino acids form looser structures, consistent with the crystal structure reported by Boudko S.P. et al [10]. The leader peptides, resembling the hooks of a triangular arrow, folds back in the opposite direction, likely due to its interaction with the non-imino acid-containing region of the triple helix. Due to the unique nature of its structure, the non-imino acid-containing region and the leader peptide may interact with other substances.

Autodock Vina is a tool for molecular docking, known for its efficiency and accuracy in predicting the binding sites and binding energies of small ligands to proteins [13]. It is widely used in drug design and biophysical research. To confirm whether SPD will binds to the candidate rhCol to form comlex ColMax, we used Autodock Vina to simulate and analyze the semi-flexible molecular docking of the 3D structure of rhCol with the ligand SPD, employing the Genetic Algorithm (GA) with 100 docking runs. As shown in Figure 3b, SPD preferentially binds to the cysteine residues at the C-terminal of rhCol through hydrogen bonds (binding energy: -6.19 kcal/mol, frequency: 18, hydrogen bond number: 4). Generally, a docking result with a binding energy less than -1.2 kcal/mol is considered feasible, and here, we selectd the lowest value. SPD can also bind to the ASP16-SER17-TYR18 of the leader peptide (Figure 3c, binding energy: -3.39 kcal/mol, frequency: 13, hydrogen bond number: 5). Other weaker binding sites were identified but are not listed here. It can be inferred that one rhCol molecule can bind to at least four SPD molecules. This preliminary binding simulation suggests the potential for complexation between the rhCol candidate and SPD molecules.

We also conducted molecular docking of rhCol with the model active molecule of EGT and found that EGT primarily binds to the GLN14 of the leader peptide through hydrogen bonds. It can also simultaneously bind to ILE30 in the triple helix region (Figure 3d, total binding energy: -3.33 kcal/mol, frequency: 5, hydrogen bond number: 2). These binding sites are distinct from those of SPD. However, the binding of EGT to the C-terminal of rhCol is relatively weak (Figure 3e, binding energy: -2.03 kcal/mol, frequency: 6, hydrogen bond number: 1). This suggests that one rhCol molecule can bind to at least three EGT molecules, with no conflict in binding sites with SPD.

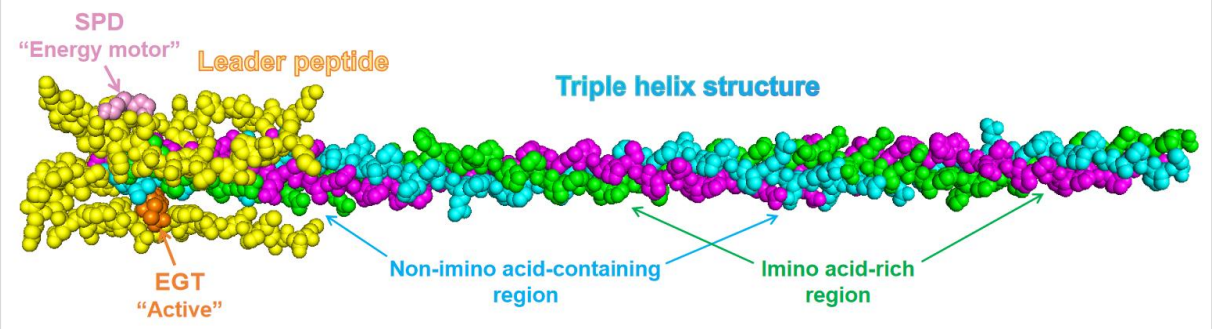


(**a**)

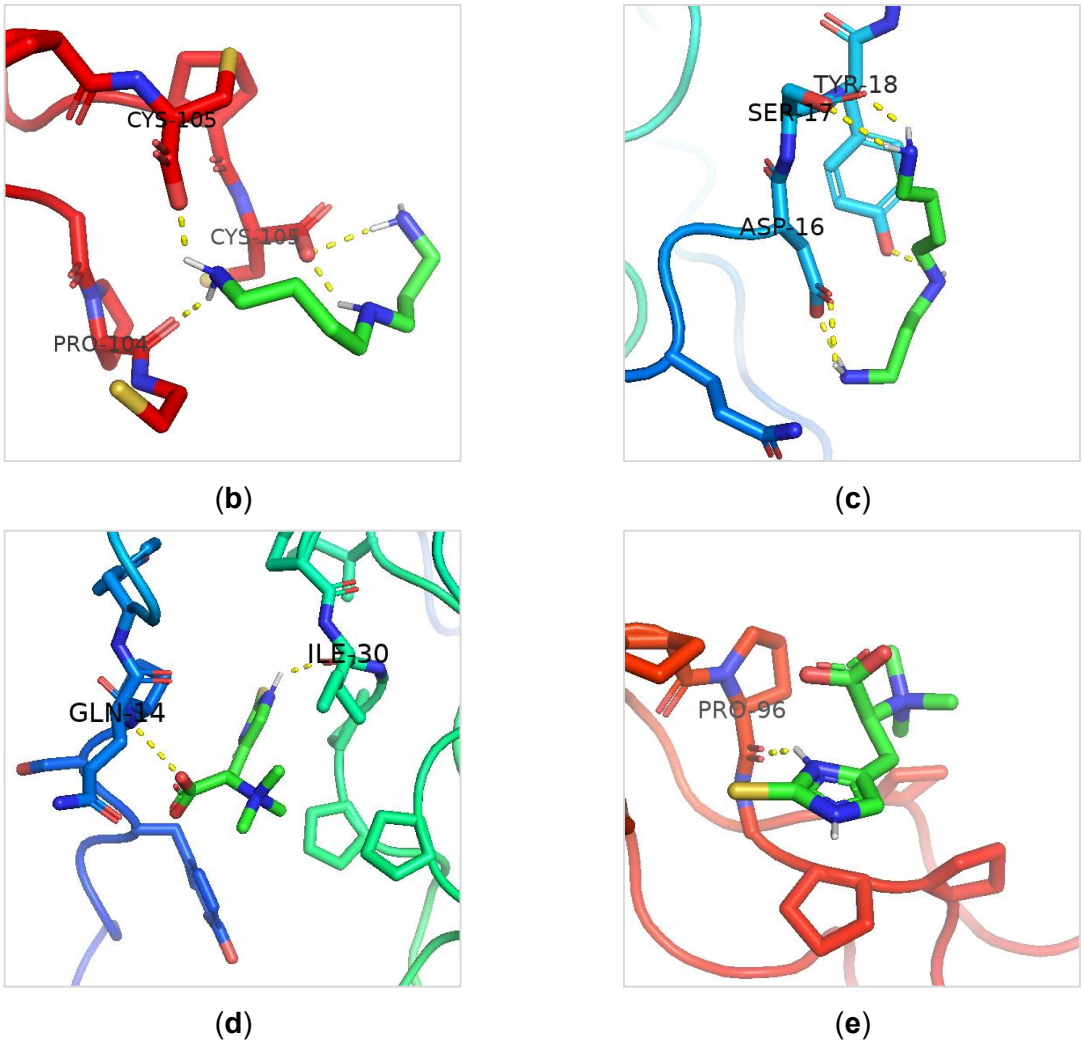


**Figure 3.** The 3D structure of rhCol and its binding sites with active molecules. (a) The 3D structure of rhCol predicted by AlphaFold3, including an example of the rhCol-SPD-EGT complex predicted by AutoDock Vina. (b) The binding site between the C-terminal of rhCol and SPD. (c) The binding site between the leader peptide and SPD. (d) The binding site between the leader peptide and EGT. (e) The binding site between the C-terminal of rhCol and EGT. Yellow lines indicate hydrogen bonds.

### *3.3. Interaction of rhCol and SPD by QCM-D*

To validate the interaction between rhCol and SPD, QCM-D measurements were conducted to investigate the real-time adsorption and desorption behaviors of rhCol from an SPD solution. As shown in Figure 4, the frequency shift (blue line) significantly decreased upon injection of the rhCol solution, indicating rapid adsorption of rhCol onto the sensor surface (light green region). Concurrently, the increased dissipation shift suggested that rhCol was adsorbed in a loose and soft manner. After introducing glycerol and Tris-HCl solution, the frequency shift increased to a steady value, indicating that the loosely adsorbed rhCol was rinsed off, reaching an adsorption equilibrium. This process also resulted in a more tightly adsorbed layer, reflected by a lower dissipation shift (light blue region). Upon injection of the SPD solution, the frequency shift further increased, suggesting that SPD molecules displaced rhCol from the adsorbing surface, thus confirming the interaction between rhCol and SPD (light red region). This interaction helped remove the loosely bound rhCol from the sensors, leaving behind a more rigid and strongly adsorbed rhCol layer, as indicated by the reduced dissipation shift (orange line). The QCM-D results validate the interaction between rhCol and

SPD, which aligns with the molecular docking predictions and suggests the potential formation of a complex supermolecule, ColMax.

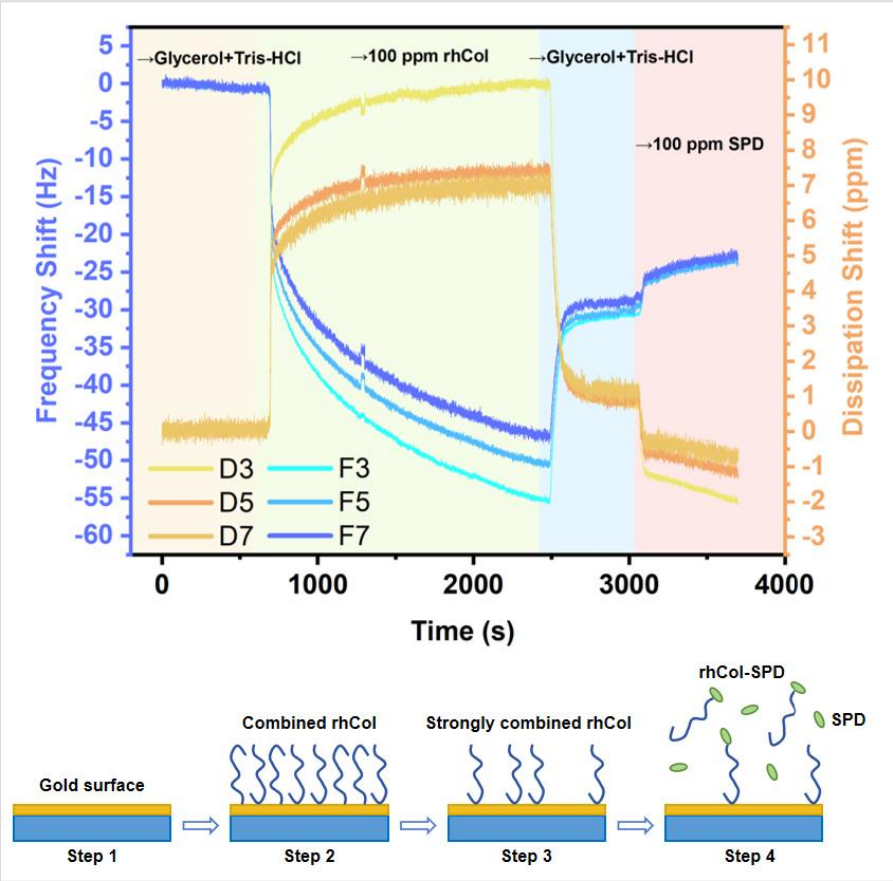


**Figure 4.** QCM-D response during the adsorption and rinse process of rhCol.

### *3.4. Synergistic Activities of rhCol-SPD-EGT*

#### *3.4.1. Autophagy*

Autophagy is a crucial cellular process by which damaged or redundant components, such as proteins and organelles, are degraded to maintain homeostasis and enable material recycling [14]. With aging, the efficiency of autophagy declines, resulting in the accumulation of cellular waste and the acceleration of cell dysfunction and tissue aging. During autophagy, the targeted substances are encapsulated by autophagic vesicles and subsequently degraded by hydrolases in lysosomes. DAPGreen, a small molecule fluorescent dye, is commonly used to detect autophagosomes and autophagolysosomes.

SPD is known to be an effective autophagy inducer that supports ATP production in cells [5, 15]. As shown in Figure 5, both collagen and SPD promoted autophagy, with SPD exhibiting a stronger effect, while EGT had no significant impact. Interestingly, when rhCol and SPD were combined to form supramolecular ColMax (formed by 100 ppm rhCol and 1 ppm SPD), the promotion of autophagy was significantly enhanced by 96% compared to the NC group, more than twice the effect of SPD alone, indicating a synergistic effect. Although the addition of EGT did not further enhance autophagy beyond the effect of supramolecule rhCol-SPD, it still resulted in a much stronger effect than EGT alone. These results suggest that the supramolecular of rhCol and SPD (ColMax) significantly boosts cellular autophagy, thereby promoting cell metabolism and maintaining healthy cellular homeostasis.

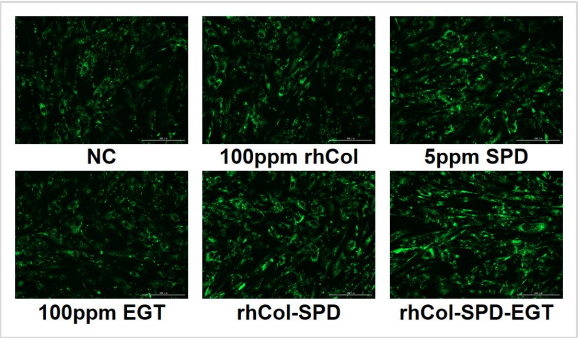


(**a**)

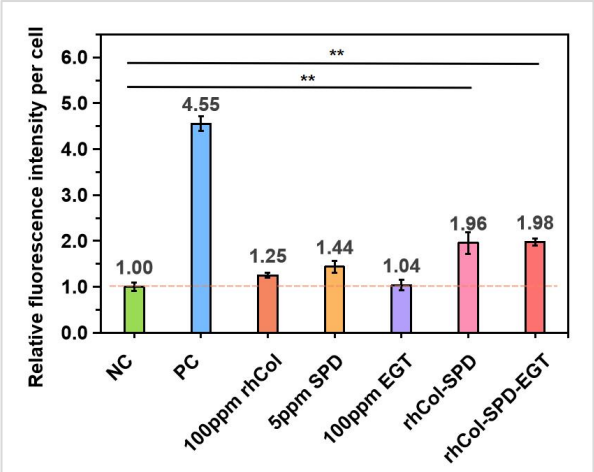


(**b**)

**Figure 5.** The effect of supramolecular collagen on cellular autophagy. (a) Representative fluorescence images showing the impact of supramolecular collagen on autophagy. (b) Quantification of relative fluorescence intensity per cell (n = 2; **p < 0.01).

*3.4.2. The Repair Effect*

There is a bidirectional vicious cycle between skin barrier damage and aging: barrier damage accelerates skin aging, while aging impairs the barrier's ability to repair itself. The cell migration assay is an important method for evaluating a sample's ability to promote barrier repair. This assay mimics the healing process of micro-wounds by creating artificial "scratches" in a monolayer of adherent cells and monitoring the dynamic changes in cell migration. As shown in Figure 6, the migration rate of rhCol-SPD-EGT (ColMax-EGT) reached 61.7%, representing a 38.2% improvement compared to the NC group and far exceeding the effects of the individual components. These results indicate that with the supramolecular ColMax (formed by 100 ppm rhCol and 1 ppm SPD), ColMax-EGT significantly promotes cell migration and skin barrier repair, thereby contributing to the delay of skin aging.

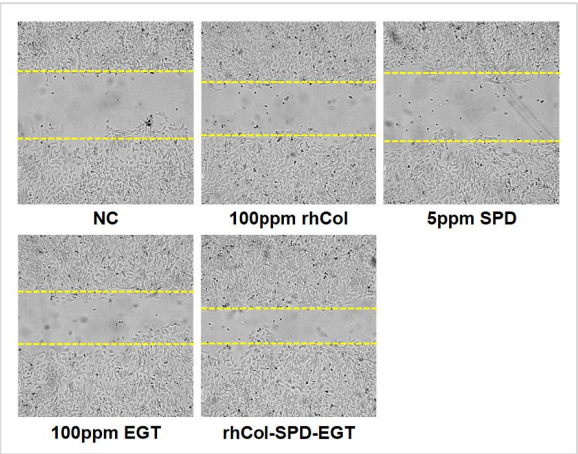


(**a**)

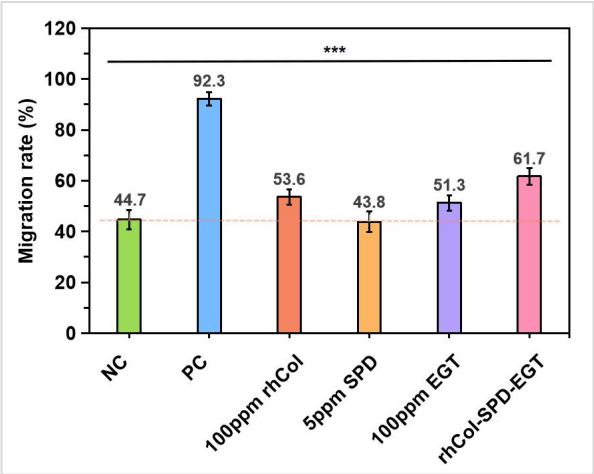


(**b**)

**Figure 6.** Cell migration rate. (a) Representative images of tested samples on cell migration. (b) Migration rate (n = 2; ***p < 0.001).

### *3.4.3. Anti-inflammation Effect*

Common environmental stimuli, such as ultraviolet radiation, microbial infections, excessive skin cleansing, allergic reactions, can trigger skin inflammation. Chronic inflammation can lead to oxidative stress, collagen degradation, and increased melanin production, ultimately resulting in wrinkles, pigmentation, and sagging. Therefore, inhibiting inflammation is crucial for regulating skin physiological aging. As shown in Figure 7, treatment with 1 ppm SPD alone did not significantly inhibit TNF-α expression compared to the model group. However, the supramolecular complex rhCol-SPD, formed by 100 ppm rhCol and 1 ppm SPD, significantly increased the inhibition rate to 54.2%. More notably, when rhCol-SPD was combined with EGT, the inhibition rate further improved to 61.4%. These results demonstrate that rhCol-SPD-EGT (ColMax-EGT) can exert anti-inflammatory and soothing effects by modulating cellular signaling pathways and suppressing TNF-α expression. Notably, the supramolecular ColMax not only exhibited superior efficacy compared to individual components but also enhanced the anti-inflammatory activity of EGT, suggesting that the synergistic supramolecular environment amplifies the overall cellular response.

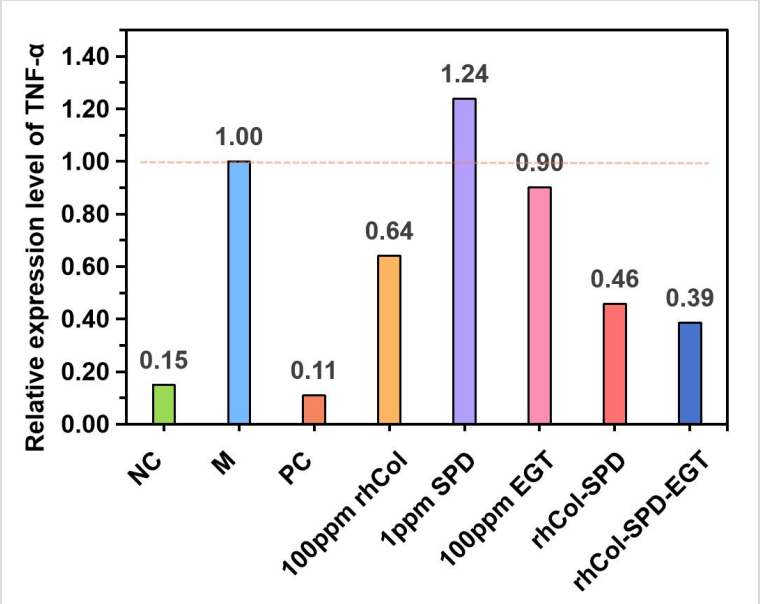


**Figure 7.** The effect of test samples on cellular inflammatory factor TNF-α expression (n = 1).

## 4. Discussion

Biomolecules play critical roles in various physiological processes due to their bioaffinity and recognition capabilities. Their superior design holds immense potential for future applications. Collagen, the most abundant protein in the human body, serves as an ideal scaffold for functionalization. In this study, we developed a unique recombinant human collagen III (rhCol) with enhanced stability and permeability, providing a versatile platform for conjugating small bioactive molecules, which has broader applications in dermatology.

We selected rhCol and SPD to form the basic supramolecular structure, rhCol-SPD (ColMax), characterized by molecular docking and QCM-D analysis. In efficacy evaluations, while SPD alone significantly promoted autophagy, ColMax demonstrated a notably stronger effect. This enhanced outcome is likely due to the supramolecular structure, where the structural support

from rhCol improves the stability, delivery efficiency, and bioavailability of SPD, amplifying its activation of cellular autophagy. Furthermore, when ColMax was combined with EGT, the resulting complex, ColMax-EGT, achieved the highest promotion of cell migration compared to rhCol, SPD, or EGT alone, indicating a strong synergistic effect. A similar synergistic enhancement was observed in anti-inflammatory assays.

These findings suggest that the rhCol-based supramolecular system, ColMax, may serve as a novel anti-aging vehicle, integrating SPD with rhCol. We speculate that SPD, acting as an autophagy activator, enables ColMax to maintain cells in a dynamic, energized state by upregulating cellular metabolism, thus enhancing overall efficacy compared to free biomolecules via a more refined physiological modulation. Moreover, the rhCol scaffold provides an optimal environment for the collaborative action of multiple small molecules. In essence, ColMax appears to orchestrate multi-pathway activation, achieving powerful biological effects by amplifying the activity of associated small molecules.

As illustrated in Figure 8, recent advances in understanding aging have revealed that aging is an integrated manifestation of complex interactions among genes, proteins, and cells [16]. The "12 hallmarks of aging" framework precisely outlines the mechanisms driving aging and offers valuable insights into potential therapeutic strategies. Disrupting any of these hallmarks accelerates aging, while the simultaneous restoration of multiple hallmarks may yield superior anti-aging effects. These hallmarks are categorized into three groups: primary, antagonistic, and integrative. Notably, the functional profile of ColMax-EGT aligns well with all three categories: for the "primary" hallmarks, ColMax-EGT significantly promotes autophagy; for the "antagonistic" hallmarks, EGT acts as a potent mitochondrial protector; and for the "integrative" hallmarks, ColMax-EGT exhibits strong anti-inflammatory activity. By targeting these three critical dimensions of aging simultaneously and leveraging the synergistic effects of collagen-based supramolecular structures, ColMax-EGT offers a comprehensive anti-aging strategy.

In summary, collagen-based supramolecular materials such as ColMax and ColMax-EGT hold great promise as innovative anti-aging ingredients. Further in-depth mechanistic studies, particularly focusing on additional small actives, are essential to fully explore and optimize their therapeutic potential.

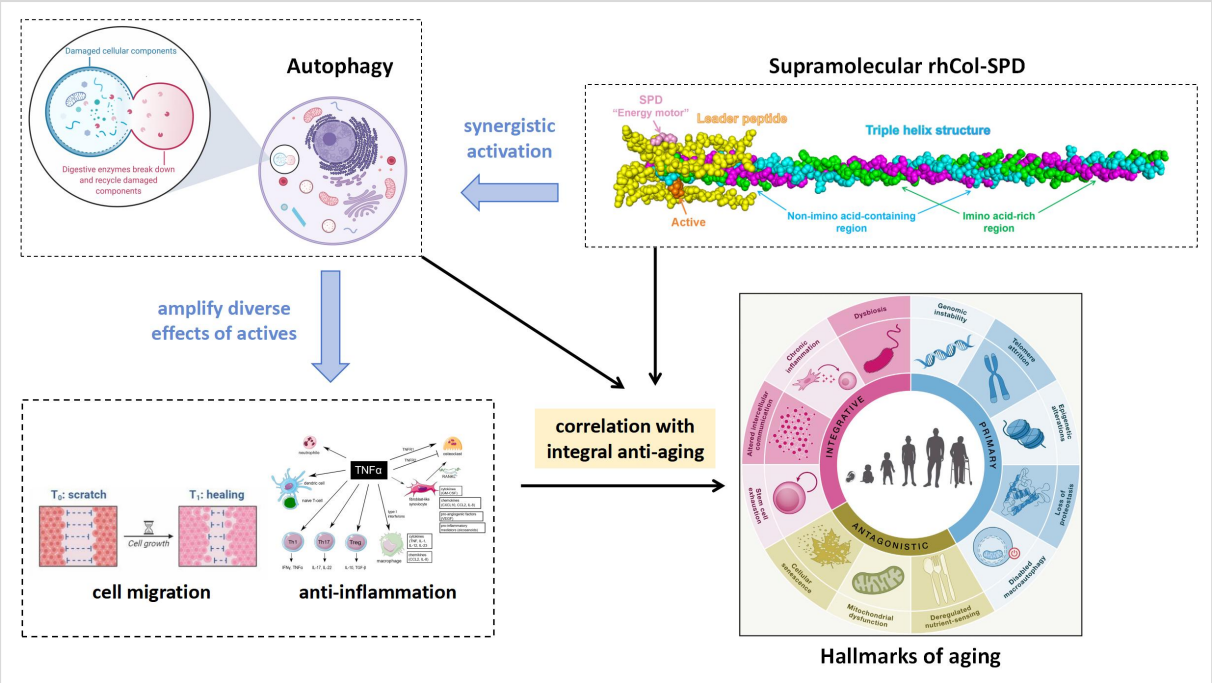


**Figure 8.** Schematic diagram of the anti-aging effect of collagen supramolecular.

## 5. Conclusion

In this study, we developed ColMax, a novel collagen supramolecular vehicle combining recombinant human collagen (rhCol) with SPD. ColMax enhanced autophagy compared to SPD alone, and when combined with EGT, it further improved cellular migration and anti-inflammatory effects. The ColMax-EGT system excels in skin barrier repair, inflammation control, and autophagy induction, delivering superior results compared to individual components. This approach paves the way for advanced cosmetic formulations that leverage the synergistic effects of collagen-based systems and small bioactive molecules, offering promising outcomes for skin care.

## 6. References

1. Shoulders M.D., Raines R.T. Collagen structure and stability. Annual review of biochemistry. 2009;78(1):929-58.
2. Datta L.P., Manchineella S., Govindaraju T. Biomolecules-derived biomaterials. Biomaterials. 2020;230:119633.
3. Chen Z., Fan D., Shang L. Exploring the potential of the recombinant human collagens for biomedical and clinical applications: a short review. Biomedical materials. 2020;16(1):012001.
4. Chen C.-X., Zhang Y.-Y., Yang J., et al. An overview of progress in the application of recombinant collagen in cosmetics. Journal of Dermatologic Science and Cosmetic Technology. 2024;1(4):100059.
5. Madeo F., Bauer M.A., Carmona-Gutierrez D., Kroemer G. Spermidine: a physiological autophagy inducer acting as an anti-aging vitamin in humans? Autophagy. 2019;15(1):165-8.
6. Ni Y.-Q., Liu Y.-S. New insights into the roles and mechanisms of spermidine in aging and age-related diseases. Aging and disease. 2021;12(8):1948.

7. Fu T.-T., Shen L. Ergothioneine as a natural antioxidant against oxidative stress-related diseases. Frontiers in Pharmacology. 2022;13:850813.
8. Brodsky B., Persikov A.V. Molecular Structure of the Collagen Triple Helix. Advances in Protein Chemistry. 70: Academic Press; 2005. p. 301-39.
9. Boudko S.P., Engel J., Bächinger H.P. The crucial role of trimerization domains in collagen folding. The International Journal of Biochemistry & Cell Biology. 2012;44(1):21-32.
10. Boudko S.P., Engel J., Okuyama K., et al. Crystal Structure of Human Type III Collagen Gly991–Gly1032 Cystine Knot-containing Peptide Shows Both 7/2 and 10/3 Triple Helical Symmetries*. Journal of Biological Chemistry. 2008;283(47):32580-9.
11. Burjanadze T.V. New analysis of the phylogenetic change of collagen thermostability. Biopolymers. 2000;53(6):523-8.
12. Abramson J., Adler J., Dunger J., et al. Accurate structure prediction of biomolecular interactions with AlphaFold 3. Nature. 2024;630(8016):493-500.
13. Eberhardt J., Santos-Martins D., Tillack A.F., Forli S. AutoDock Vina 1.2.0: New Docking Methods, Expanded Force Field, and Python Bindings. Journal of Chemical Information and Modeling. 2021;61(8):3891-8.
14. Glick D., Barth S., Macleod K.F. Autophagy: cellular and molecular mechanisms. The Journal of Pathology. 2010;221(1):3-12.
15. Madeo F., Eisenberg T., Pietrocola F., Kroemer G. Spermidine in health and disease. Science. 2018;359(6374):eaan2788.
16. López-Otín C., Blasco M.A., Partridge L., et al. Hallmarks of aging: An expanding universe. Cell. 2023;186(2):243-78.